Evaluation of E-Beam Repair for Nanoimprint Templates

Marcus Pritschow*[a], Volker Boegli[b], Joerg Butschke[a], Mathias Irmscher[a], Douglas Resnick[c], Holger Sailer[a], Kosta Selinidis[c], Ecron Thompson[c]
[a] IMS Chips, Allmandring 30a, D-70569 Stuttgart, Germany
[b] NaWoTec GmbH – A Carl Zeiss SMT Company, Industriestr. 1, D-64380 Rossdorf, Germany
[c] Molecular Imprints, Inc., 1807-C West Braker Lane, Austin, TX 78758, USA

ABSTRACT

Two essential process steps of the template fabrication chain are inspection and repair. The widely introduced gas assisted e-beam etching and deposition technique for mask repair offers crucial advantages, especially regarding the resolution capability. We started the evaluation of a new e-beam repair test stand based on the Zeiss MeRiT technology for UV-NIL template repair. For this purpose, templates with programmed defects of different shapes and sizes have been designed and fabricated. The repair experiments were focused on the development of recipes for quartz etching and deposition specifically tailored for NIL repair requirements Both, clear and opaque programmed defects have been repaired and the results have been analyzed. After recipe optimization, templates with repaired programmed defects have been imprinted on a Molecular Imprints Imprio 250 tool. By comparing template and imprint results we investigated the repair capability.

Keywords: Nanoimprint Lithography, Template, Repair

1. INTRODUCTION

UV nanoimprint lithography (UV-NIL) has been proved as an effective technology for the replication of nanometer-scale structures, and industrial applications for the production of patterned media or photonic crystals are known, so far [1]. In addition, UV-NIL is considered a candidate for the fabrication of CMOS devices and has been included in the ITRS roadmap as an option for the 32nm node and below. Consortia world-wide are evaluating UV-NIL for this purpose and the development of the infrastructure for imprint processing and template fabrication has been started [2]. Recently, remarkable progress has been achieved in template patterning. Using state-of-the-art pattern generators and commercially available resists and etching tools, templates with real gate designs could be realized with specifications approaching the 32nm node requests in terms of resolution, line edge roughness, placement, and uniformity [3].

In UV-NIL high-resolution patterns etched into the template are replicated into a monomer layer deposited on a substrate. Pattern defects resulting from the e-beam patterning and subsequent pattern transfer processes significantly contribute to imprint defectivity [4]. Thus inspection and repair are two essential components of the template fabrication chain. Compared to other mask repair technologies the widely introduced gas assisted e-beam etching and deposition technique for photomask repair offers crucial advantages, especially regarding the resolution capability [5]. The potential as a repair technique for 45nm generation photomasks has been demonstrated [6] and is therefore a viable approach for the repair of 1X nanoimprint patterns. In contrast to the 4X lithography technology of binary and phase shift photomasks the requirements in terms of resolution and placement are challenging. Furthermore, existing repair technologies are not faced with a direct contact of the repaired imprint mask to polymer materials or anti-adhesion agents. Additionally, an exact reproduction of the defective 3D relief structure pattern is necessary.

We started the evaluation of a new e-beam repair test stand based on the Zeiss MeRiT technology for high-resolution UV-NIL template repair. For this purpose templates with programmed defects of different shapes and sizes have been designed and fabricated and imprints of repaired defects have been performed. The investigated defects consist of protrusion and hollow type quartz defects, which correspond to opaque and clear defects on phase shift photomasks.

* pritschow@ims-chips.de, phone: +49-711-21855-420, fax: +49-711-21855-7420

Photomask Technology 2008, edited by Hiroichi Kawahira, Larry S. Zurbrick,
Proc. of SPIE Vol. 7122, 71222L · © 2008 SPIE · CCC code: 0277-786X/08/$18 · doi: 10.1117/12.801946

2. EXPERIMENTAL

2.1 Methodology

The target of this work was to evaluate the e-beam repair tool capability for nanoimprint patterns with focus on the development of recipes for quartz etching and deposition specifically tailored for NIL repair requirements. For this purpose we fabricated programmed defect patterns on 6-inch quartz masks. Various repair cycles on clear and opaque programmed defects have been performed to set up appropriate tool and process parameters, and the results have been analyzed using SEM inspection. Imprints of the repaired imprint mask in a thick monomer have been conducted at Molecular Imprints (Austin, TX, USA). This allows the inspection of repaired pattern imprints without any impact of an interface between monomer and substrate material. After successful demonstration of the tool setup, we performed a second experimental loop, where the repair processes including optimized process parameters have been applied to programmed defect patterns on a 65×65mm^2 quartz template. For this purpose a 3-to-6-inch adapter has been designed and manufactured for the repair tool stage. Imprints of the repaired template with a Molecular Imprints Imprio 250 tool on 300mm silicon wafers were used to evaluate the repair process.

2.2 Template fabrication process

The template fabrication sequence uses similar processes developed for the fabrication of phase shift photomasks [7]. The process flow is depicted schematically in Fig. 1. Usually, four templates are fabricated at once on a standard 6-inch 6025 fused silica quartz blank with a 10nm chromium layer. A chemically amplified positive tone resist (pCAR) was coated and exposed using a variable shape e-beam writer Vistec SB352HR, operating at 50kV and a beam current density of 20A/cm^2. Pattern transfer into the Cr film was accomplished using a Cl_2/O_2-based dry etch process. Subsequently, the Cr was used as a hardmask during a fluorine-based dry etch process to define quartz structures with a depth of 110nm. Chrome and quartz etching was done in an Oerlikon mask etch tool equipped with Gen III & Gen IV etch chambers. A mesa etch to define the imprint areas as well as a dice and polish step used to separate the plate into four distinct templates finalizes the process sequence.

2.3 Programmed defect pattern

A template pattern with programmed defects was designed for this repair study consisting of different types of defects (Fig. 2). They are suitable for both additive and subtractive repair processes. Their size was systematically varied allowing the determination of the repair capability limit. An overview of the different programmed defects is given in Table 1. The detection of small random defects is a challenging task. For this reason defective cells, which can be reliably identified, were periodically embedded into an array of non-defective cells. Non-defective cells were used as reference cells for the e-beam repair process. Additionally, a set of identical defects facilitates the parameter adjustment of the repair processes.

Repair Type	Programmed Defect Type	Dimension Change
Deposition	1-dimensional extension	Fixed width = 100 nm. Height increases by 10 to 150 nm in 5 nm increments
	2-dimensional extension	Width = height and increases by 10 to 150 nm in 5 nm increments
	Isolated extension	Fixed width = 100 nm. Height increases by 10 to 150 nm in 5 nm increments
Etching	Shrinking contact	Width = height and reduces by 0 to 58 nm in 2 nm increments
	Line-end shortening	Height fixed at feature size. Width reduces by 0 to 145 nm in 5 nm increments
	1-dimensional mouse bite	Fixed width = 100 nm. Height increases by 4 to 116 nm in 4 nm increments
	2-dimensional mouse bite	Width = height and increases by 4 to 116 nm in 4 nm increments
	Internal mouse bite	Fixed width = 100 nm. Height increases by 4 to 116 nm in 4 nm increments

Table 1. Dimensional variation of programmed defects.

2.4 E-beam repair

The repair experiments have been performed on a new test stand based on the Zeiss MeRiT technology, which utilizes e-beam induced etch and deposition processes. When a defect is located on the substrate, suitable precursor gases are dispensed in very close vicinity to the incident electron beam. Depending on the precursor chemistry, a reaction is induced by the focused electron beam. This leads to a deposition caused by fragmentation of precursor molecules or an

etch reaction between the absorbed molecules and the substrate material, resulting in volatile products. Since the reaction is confined only to the area exposed by the electron beam, this technique allows high-resolution nanostructuring [5]. The repair structure is derived by comparing a high-resolution image of the defective area with the same image of a non-defective area. The repair shape is generated as the difference of these two images, and adjusted for processing purposes. Since imperfection of a pattern can be mistakenly identified as a defect, alternatively the reference can be generated using information taken from the original gds-design file [8]. The quality of the repair does not only depend on the reference image, but also on the precise beam placement on the defective area.

There are several requirements for the repair process when applied to nanoimprint templates. Deposited material to repair opaque defects has to be transparent to UV light and has to exhibit good adhesion to the substrate. Otherwise material delamination can occur during the imprint process, e.g. due to impact of the imprint monomer, anti-adhesion agents or high imprint forces. One of the advantages of using e-beam for quartz removal is that etching can be made in small trenches with excellent profile control. On the other hand, the process has to be well adjusted to allow the removal of an accurate amount of material without removing surrounding material. This can cause a deviating geometry between the repaired and the reference structure.

3. RESULTS AND DISCUSSION

3.1 Repair setup loop on 6-inch quartz plate: repair and imprint results

The first experiments for a basic setup of the repair tool have been done with programmed defects fabricated on a 6-inch quartz plate. Fig. 3 shows SEM images of standard cell test patterns with 1D and 2D extension, line-end shortening and 1D mouse bite, representing opaque and clear defects. The repair area was correctly detected by applying the pattern copy method using a reference image of a non-defective cell, and the repair processes could be successfully conducted. Fig. 4 shows the same defect pattern in Fig. 3 after repair by e-beam induced deposition and etching, respectively. A wide range of defects have been investigated to find optimum repair parameters for the later template repair. Precise beam placement and the accurate setting of the repair shape are important for high-resolution defect repair. In addition, etch depth and deposition height, respectively, need to be carefully determined in order to allow the reconstruction of a defective pattern with the original shape and size of a non-defective pattern. The repair processes can be tuned by three parameters: deposition time, etch time and edge bias. The effect of parameter optimization loops on 2D extension defects with varied deposition times and edge bias applied to the repair area and corresponding imprint results are shown in Fig. 5. If the deposition time is chosen too short, the defect cannot be completely filled up and will lead to remaining polymer after imprint. As a consequence, a spacer can occur after pattern transfer into the substrate material. In UV-NIL these residues can cause severe problems as they are directly replicated into the monomer. On the other hand, when the deposition time is set too long, the resulting imprint shows a dent in the resist (Fig. 5a). In case of an imprint process utilizing a substrate covered with a thin monomer, this embossed structure can lead to insufficient template contact of the adjacent imprint patterns. The edge bias allows a fine-tuning of the repair area position in a very narrow range. Sloped sidewalls can be compensated and a better filling of trenches can be achieved (Fig. 5b). It was found, that these parameters had to be adjusted for each defect type to achieve good repair performance. Imprint results have also shown that all repaired defects were clearly imprinted and were not damaged during the imprint process. No delamination could be observed and the deposited material exhibited good adhesion to the quartz (Fig. 6). These results show the feasibility of the e-beam repair process for 3D nanoimprint patterns. In a next step, we performed repair experiments on a real template.

3.2 Optimized loop on 65×65mm^2 quartz template: repair and imprint results

Experiments with optimized repair tool parameters have been done with programmed defects fabricated on a 65×65mm^2 quartz template. Fig. 7 shows SEM images of programmed defects consisting of 2D extension, line-end shortening, shrinking contact and 2D mouse bite. Additionally, the template pattern contains internal mouse bite defects. The template was cleaned and imprinted into a 125nm thin layer of low viscosity monomer on a 300mm silicon wafer followed by UV curing. Fig. 8 shows the same defect pattern in Fig. 7 after repair and the corresponding imprint patterns. The imprint results show the exact replication of the repaired template and no problems regarding the UV hardening or the release step could be observed. In addition, no impact of surface or line edge roughness due to the etch repair process could be seen on the template.

Since the automatic defect detection capability of the software version was limited to minimum feature size of 50nm, manual adjustments were done instead. By carefully selecting repair parameters including deposition time, etch time and edge bias, we were able to repair mouse bite defects (Fig. 9 and 10) and 2D extension defects (Fig. 11) with defect size down to 30nm. Repair experiments on internal mouse bite defects in Fig. 9 revealed that etch time during repair can be longer without affecting the imprint result. On the other hand if the etch time is too short the resist is thinner at this point and can cause a selectivity problem during pattern transfer. The durability of a repaired template is very important for applying UV-NIL to mass production. We demonstrated over 600 uses of the repaired template without pattern degradation. A comparison of the imprint pattern after the first and after 600 uses of the template is shown in Fig. 12. These results indicate that e-beam repair is suitable for repeated application in UV-NIL.

4. CONCLUSION

Programmed defects of different shapes and sizes have been designed and fabricated. The repair experiments have been focused on the development of recipes for quartz etching and deposition specifically tailored for NIL repair requirements. A wide range of clear and opaque programmed defects have been repaired and the results have been analyzed using SEM inspection. After recipe optimization, templates with repaired programmed defects have been imprinted on 300mm silicon wafers using a Molecular Imprints Imprio 250 tool. By comparing template and imprint results we investigated the repair capability and no problems regarding adhesion and UV transparency of the deposited material could be observed. With optimized parameters repair of defect sizes down to 30nm has been demonstrated. It was found that suitable repair strategies are necessary due to the large variety of defect shapes and sizes. This might include the application of repeated repair cycles on the same defect area or a separation of the repair area and application of different repair parameter settings to compensate for nonuniform defect shapes. E-beam repair with its advantages of precise beam placement using fine resolution images and damage free repair by e-beam induced chemical reactions is a promising repair technology for high-resolution UV-NIL templates. Further systematic investigations are planned using arrays of typical programmed defects with identical sizes, which are more suitable for adjustment of the repair processes. In addition, an improved test stand based on the Zeiss MeRiT technology will be used in order to repair smaller defects.

5. ACKNOWLEDGMENTS

The authors would like to thank Petra Spies from NaWoTec GmbH for performing e-beam template repair. This work has been supported by the MEDEA+ 2T305 FANTASTIC project, the German Federal Ministry for Education and Research and by the Ministry of Economic Affairs of Baden-Wuerttemberg.

REFERENCES

[1] M. Melliar-Smith, “Lithography beyond 32nm: a role for imprint”, Proc. SPIE 6517, Plenary Paper (2007).
[2] I. Yoneda, S. Mikami, T. Ota, T. Koshiba, M. Ito, T. Nakasugi, and T. Higashiki, “Study of nanoimprint lithography for applications toward 22nm node CMOS devices”, Proc. SPIE 6921, 692104 (2008).
[3] J. Yeo, H. Kim, and B. Eynon, “Full-field imprinting of sub-40 nm patterns”, Proc. SPIE 6921, 692107 (2008).
[4] I. McMackin, J. Perez, K. Selenidis, J. Maltabes, D. Resnick, and S.V. Sreenivasan, “High resolution defect inspection of step and flash imprint lithography for 32 nm half-pitch patterning”, Proc. SPIE 6921, 69211L (2008).
[5] T. Liang, E. Frendberg, D. Bald, M. Penn, and A. Stivers, “E-beam mask repair: fundamental capability and applications”, Proc. SPIE 5567, 456 (2004).
[6] S. Kanamitsu, K. Morishita, and T. Hirano, “Application of EB repair tool for 45-nm generation photomasks”, Proc. SPIE 6607, 66072M (2007).
[7] M. Irmscher, J. Butschke, G. Hess, F. Letzkus, M. Renno, H. Sailer, H. Schulz, A. Schwersenz, E. Thompson, and B. Vratzov, “Template manufacturing for nanoimprint lithography using existing infrastructure”, Proc. SPIE 5992, 59922E (2005).
[8] V. Boegli, N. Auth, and U. Hofmann, “Mask repair using layout-based pattern copy for the 65 nm node and beyond”, Proc. SPIE 6349, 63491G (2006).

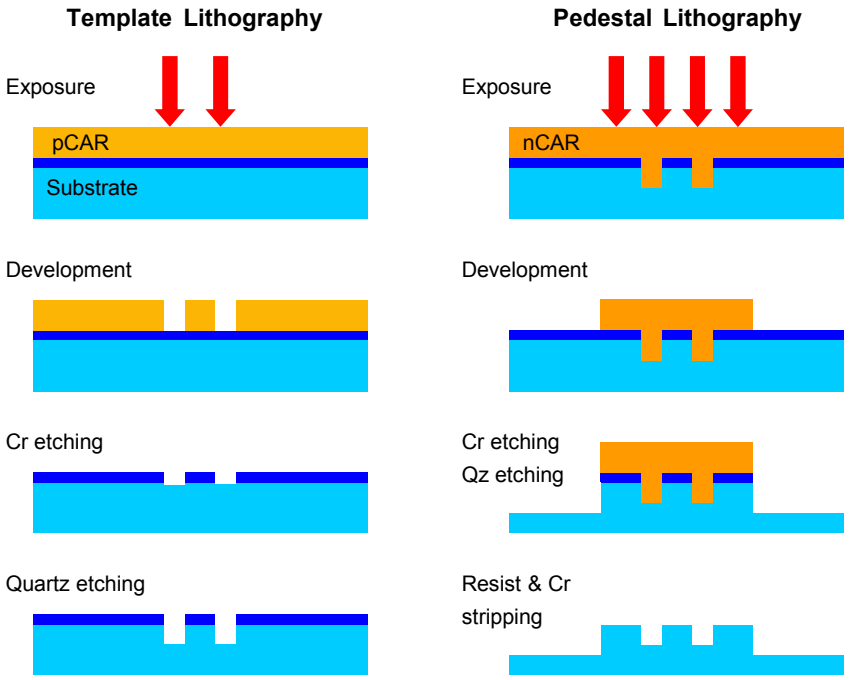

Fig. 1. Template process sequence for fabricating the programmed defect patterns.

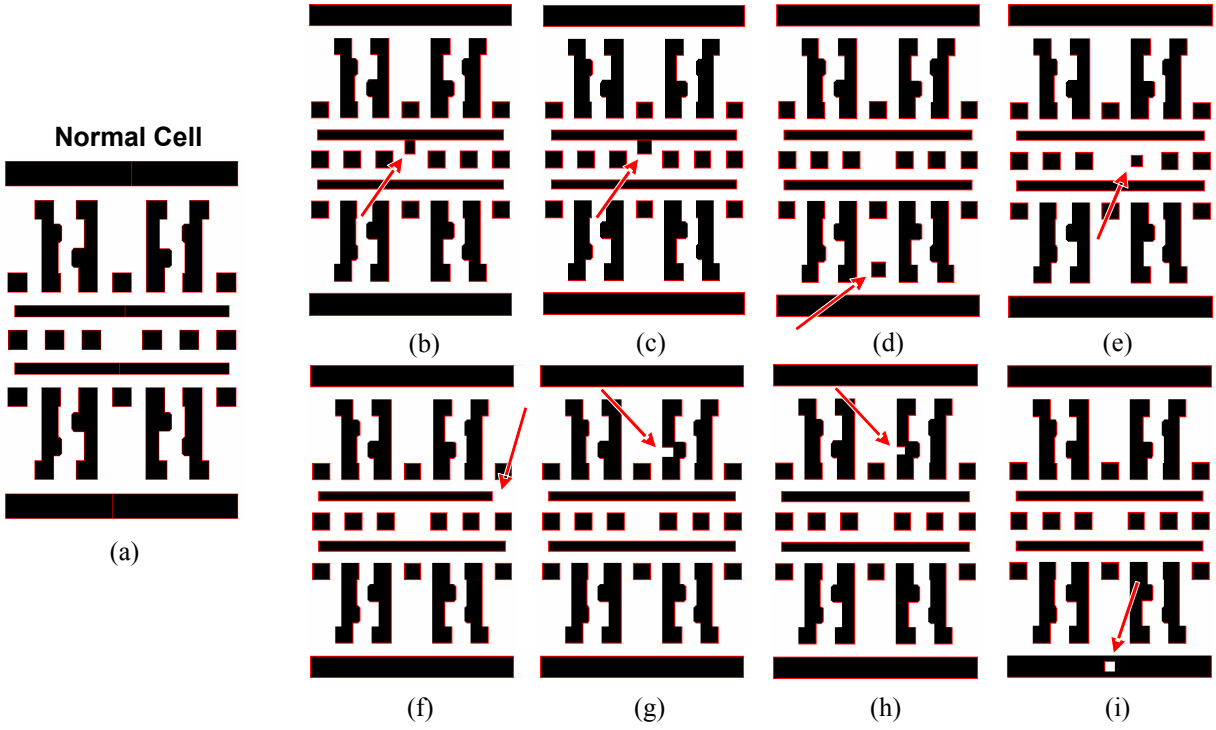

Fig. 2. Different types of programmed defects: (a) Reference cell, (b) 1-dimensional extension, (c) 2-dimensional extension, (d) isolated extension, (e) shrinking contact, (f) line-end shortening, (g) 1-dimensional mouse bite, (h) 2-dimensional mouse bite, (i) internal mouse bite.

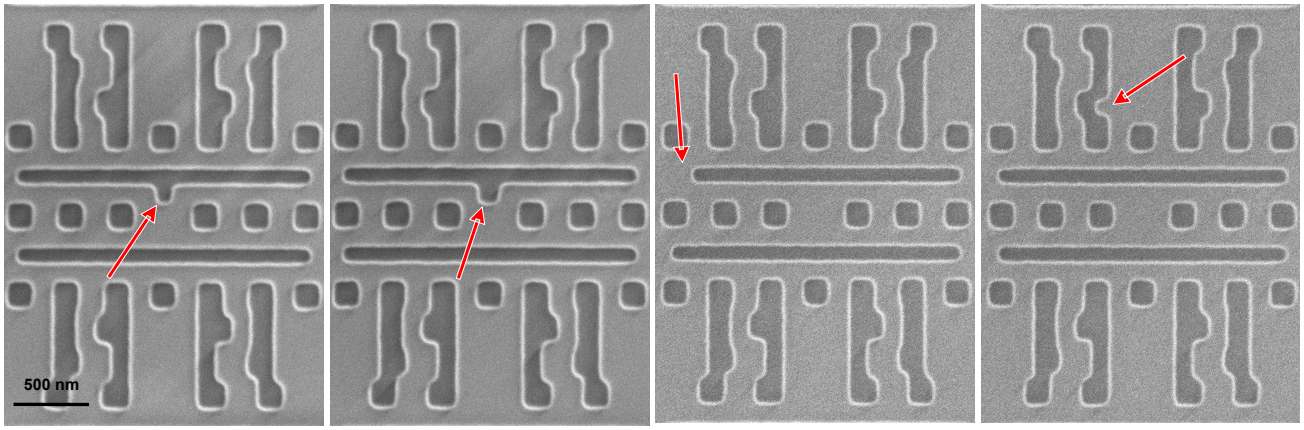

(a) (b) (c) (d)

Fig. 3. Programmed defect pattern fabricated on a 6-inch quartz plate for initial repair tool setup: (a) 1-dimensional extension, (b) 2-dimensional extension, (c) line-end shortening, (d) 1-dimensional mouse bite.

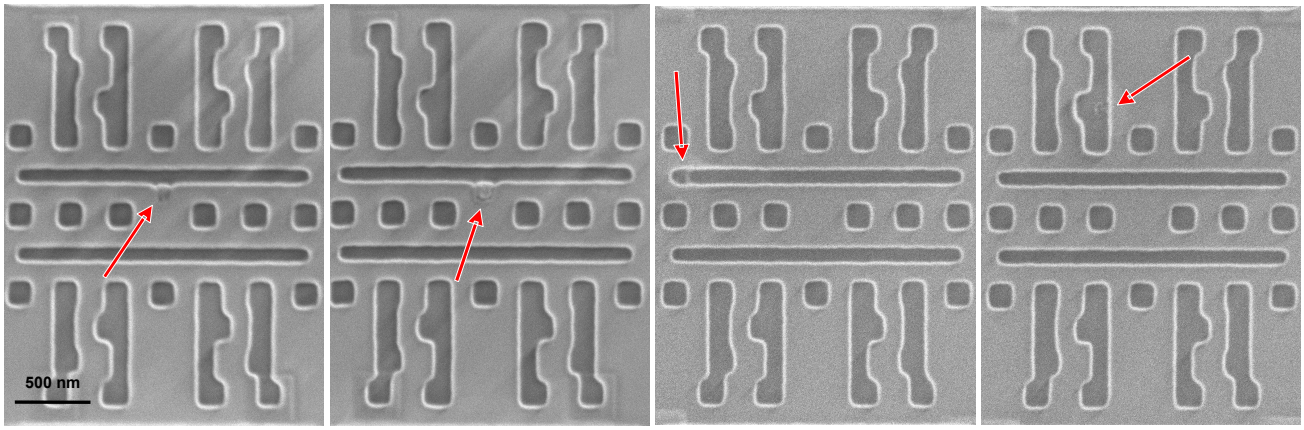

(a) (b) (c) (d)

Fig. 4. Programmed defects repaired by e-beam induced deposition (a)+(b) and e-beam induced etching (c)+(d).

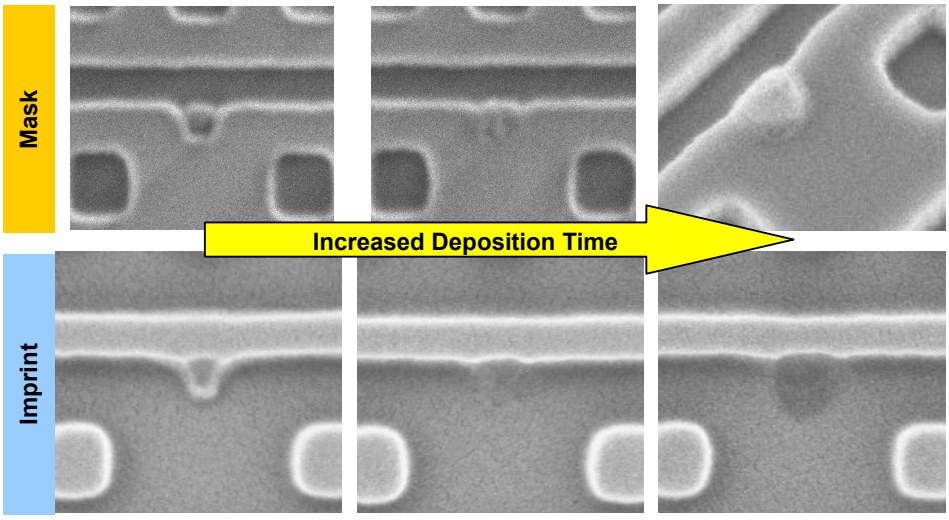

(a)

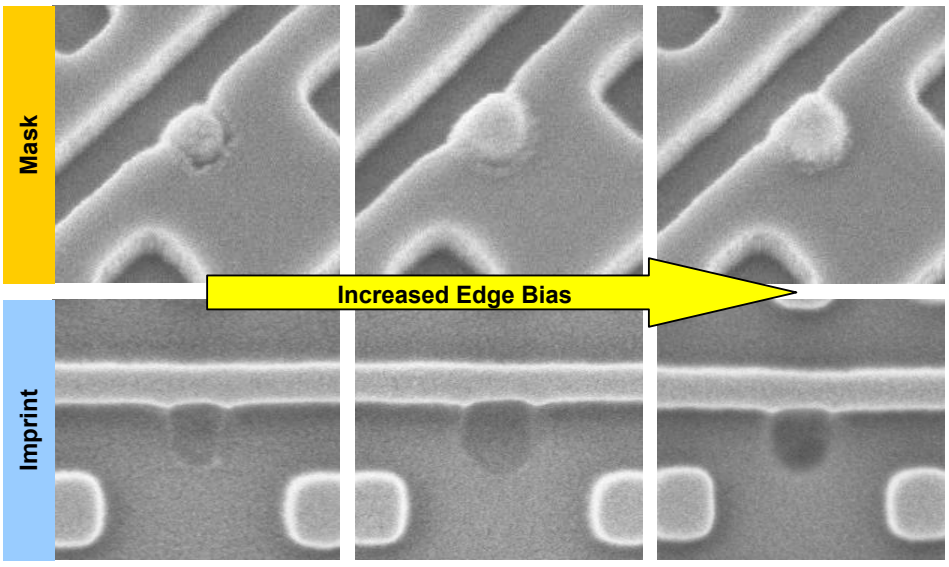

(b)

Fig. 5. Repair cycle of 2-dimensional extension defects by e-beam induced deposition with varying deposition time (a) and edge bias (b), and corresponding imprint results.

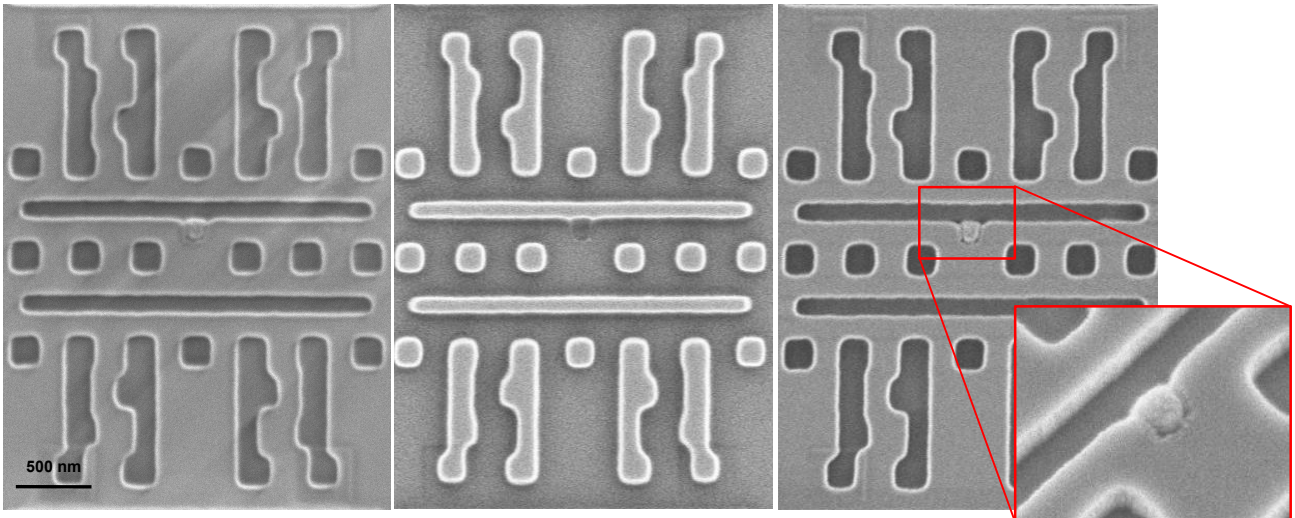

(a) (b) (c)

Fig. 6. Repaired 2-dimensional extension defects on a 6-inch quartz mask: (a) before imprint, (b) corresponding imprint result, and (c) the same defect pattern in quartz after imprint.

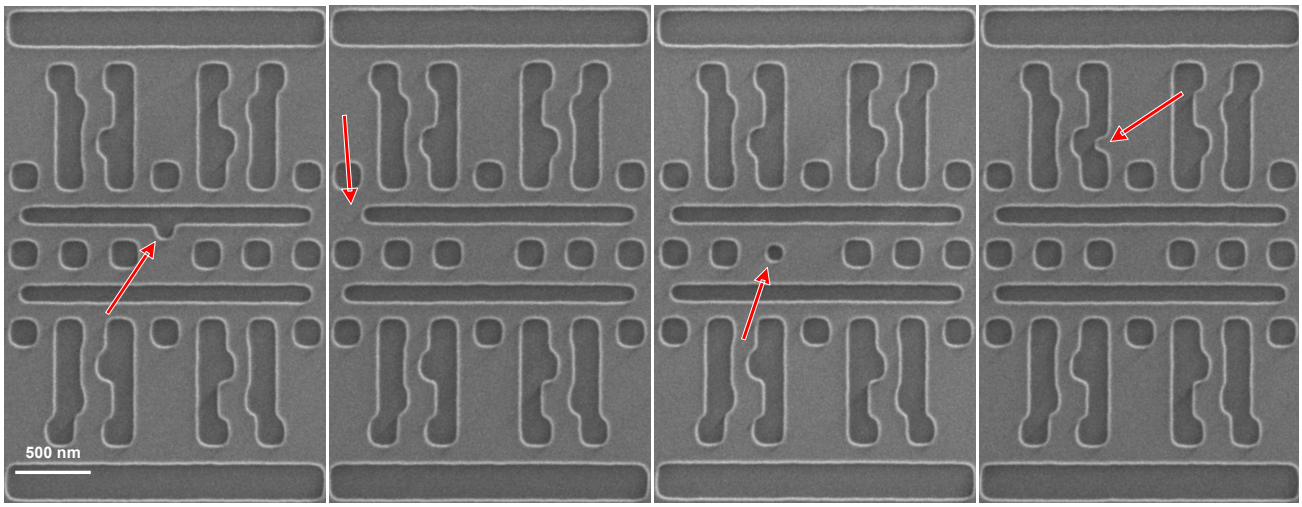

(a) (b) (c) (d)

Fig. 7. Programmed defect pattern fabricated on a 65×65mm^2 quartz template: (a) 2-dimensional extension, (b) line-end shortening, (c) shrinking contact, (d) 2-dimensional mouse bite.

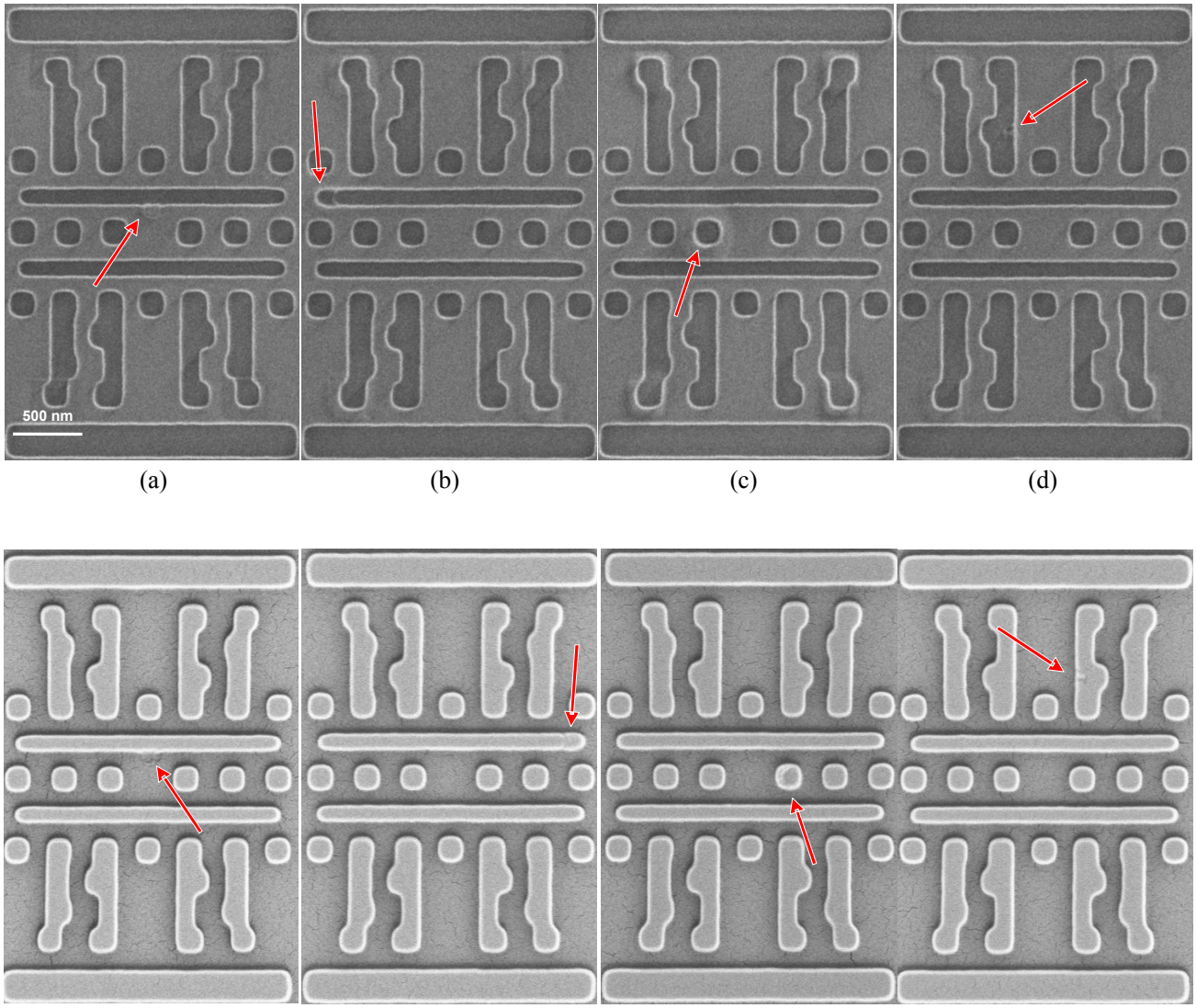

Fig. 8. Programmed defect pattern repaired by e-beam induced deposition (a), e-beam induced etching (b)-(d), and corresponding imprint results (e)-(h).

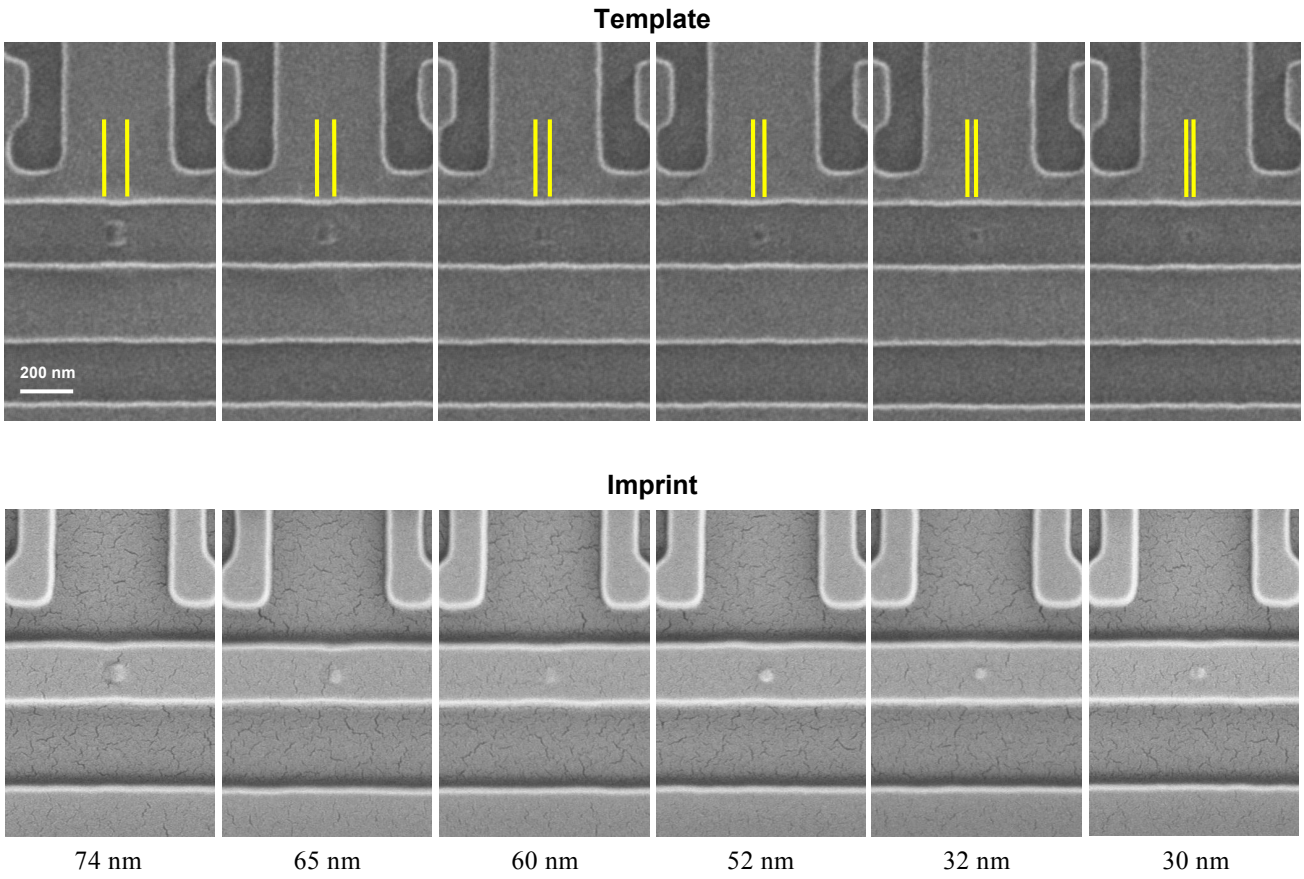

Fig. 9. Repair results of internal mouse bite defects by e-beam induced etching with optimized parameter settings and corresponding imprint results. A minimum defect size down to 30nm could be repaired with manual parameters.

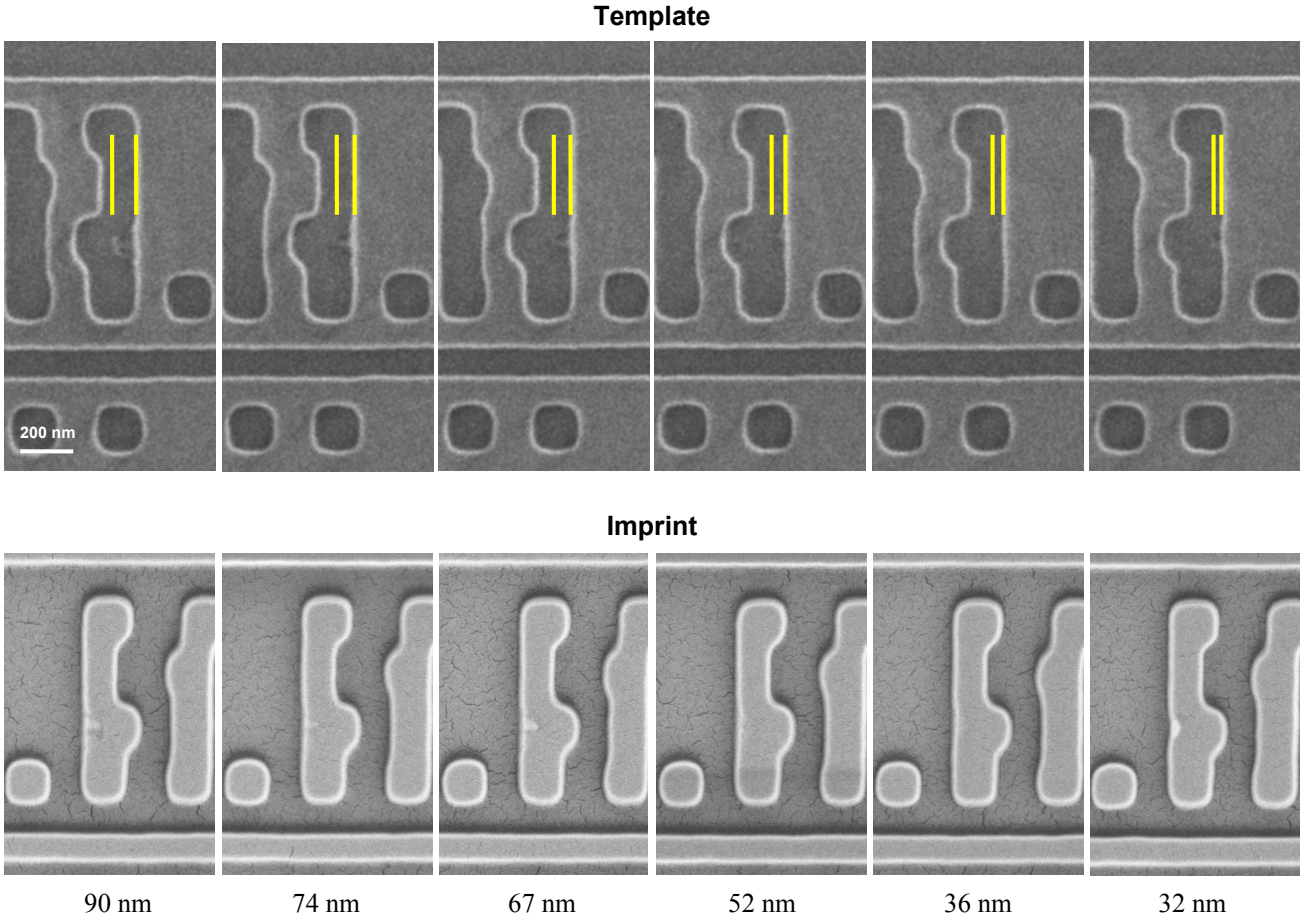

Fig. 10. Repair results of 2-dimensional mouse bite defects by e-beam induced etching with optimized parameter settings and corresponding imprint results. A minimum defect size down to 32nm could be repaired with manual parameters.

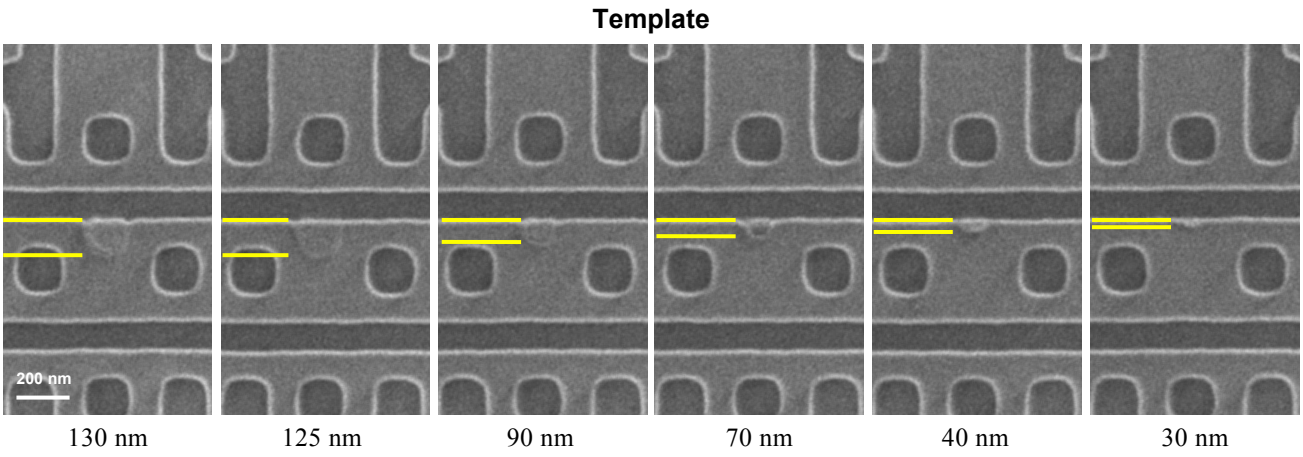

Fig. 11. Repair results of 2-dimensional extensions by e-beam induced deposition with optimized parameter settings. Minimum defect sizes down to 30nm could be repaired with manual parameters.

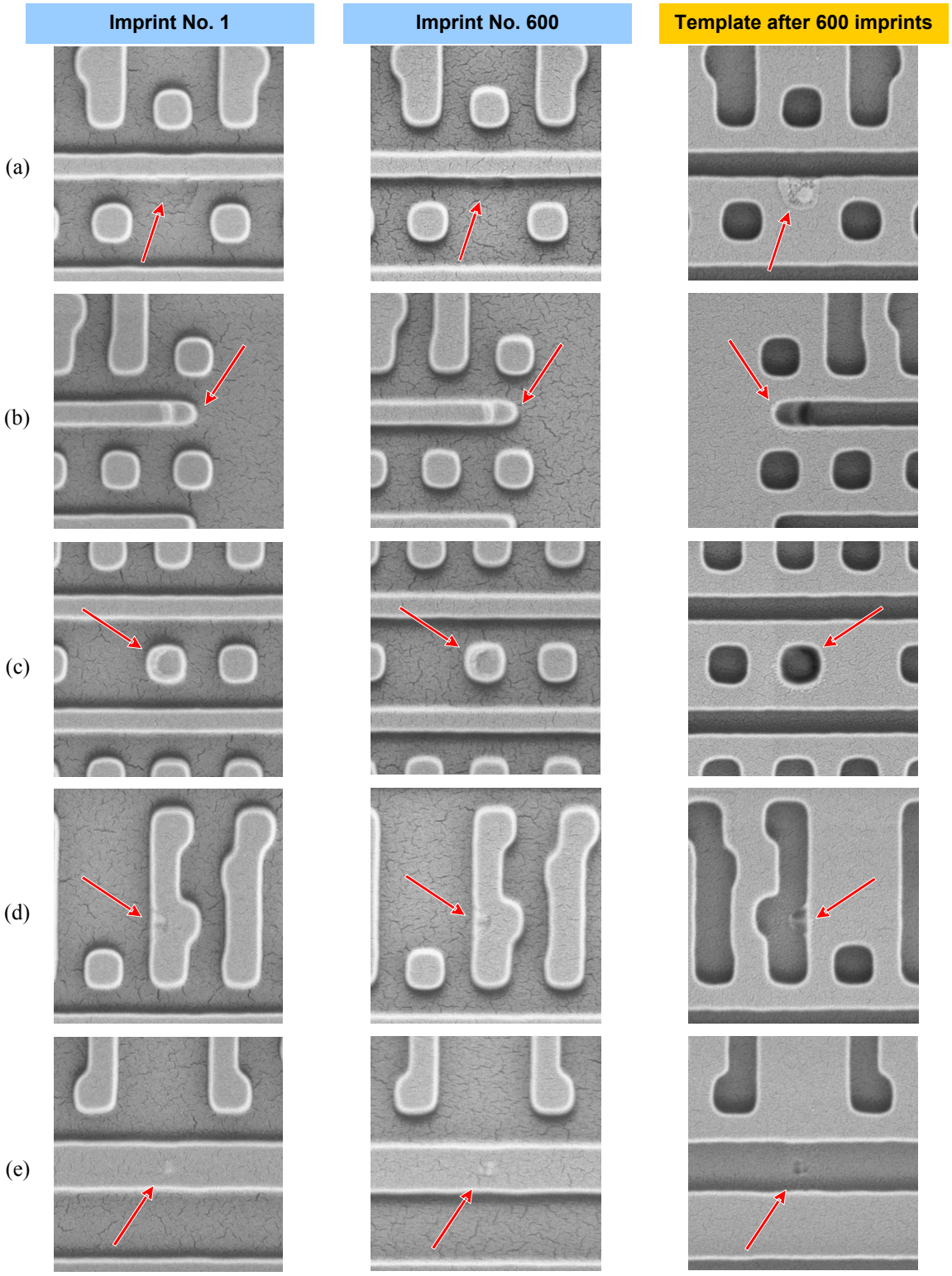

Fig. 12. Imprint results of repaired defects after first use and 600 repeated uses of the template: (a) 2-dimensional extension, (b) line-end shortening, (c) shrinking contact, (d) 2-dimensional mouse bite, (e) internal mouse bite.